Tyrosine Nitration of IκBα: A Novel Mechanism for NF-κB Activation[†,‡]

Vasily A. Yakovlev,[§] Igor J. Barani,[§] Christopher S. Rabender,[§] Stephen M. Black,[∥] J. Kevin Leach,[⊥] Paul R. Graves,[§] Glen E. Kellogg,[@] and Ross B. Mikkelsen*[,§]

Department of Radiation Oncology, Massey Cancer Center, Virginia Commonwealth University, Richmond, Virginia 23298, Vascular Biology Center, Medical College of Georgia, Augusta, Georgia 30912, Department of Medicinal Chemistry, Virginia Commonwealth University, Richmond, Virginia 23298, and Drug Metabolism and Pharmacokinetics, Merck Research Laboratories, Boston, Massachusetts 02115

Received June 5, 2007; Revised Manuscript Received August 7, 2007

ABSTRACT: The NF-κB family of transcription factors is an important component of stress-activated cytoprotective signal transduction pathways. Previous studies demonstrated that some activation mechanisms require phosphorylation, ubiquitination, and degradation of the inhibitor protein, IκBα. Herein, it is demonstrated that ionizing radiation in the therapeutic dose range stimulates NF-κB activity by a mechanism in which IκBα tyrosine 181 is nitrated as a consequence of constitutive NO• synthase activation, leading to dissociation of intact IκBα from NF-κB. This mechanism does not appear to require IκBα kinase-dependent phosphorylation or proteolytic degradation of IκBα. Tyrosine 181 is involved in several noncovalent interactions with the p50 subunit of NF-κB stabilizing the IκBα−NF-κB complex. Evaluation of hydropathic interactions of the IκBα−p50 complex on the basis of the crystal structure of the complex is consistent with nitration disrupting these interactions and dissociating the IκBα−NF-κB complex. Tyrosine nitration is not commonly studied in the context of signal transduction. However, these results indicate that tyrosine nitration is an important post-translational regulatory modification for NF-κB activation and possibly for other signaling molecules modulated by mild and transient oxidative and nitrosative stresses.

Members of the Rel/NF-κB family of transcription factors mediate cellular responses to oxidative and other stresses (*1*). NF-κB transcription factors are formed by the homo- or heterodimerization of proteins of the Rel family, including p50, p52, p65 (RelA), c-Rel, and RelB. The most abundant and best-understood dimer is the p65−p50 dimer. This dimer exists in the cytoplasm complexed with an inhibitor protein, IκBα, that masks the NF-κB nuclear localization sequence (*2*). Stimulation of cells with cytokines such as tumor necrosis factor (TNFα)[1] results in the phosphorylation, ubiquitination, and degradation of IκBα, permitting the unmasked p65−p50 heterodimer to translocate into the nucleus (*2*).

Ionizing radiation (IR) also activates NF-κB by mechanisms not fully understood. At high IR doses (>10 Gy), activation appears similar to that observed for TNFα. DNA damage-inducible kinases, ATM and DNA-PK, activate IκBα kinases (e.g., IKKβ), stimulating the phosphorylation, ubiquitination, and proteasome degradation of IκBα (*1*, *3*). IKKβ activity and IκBα degradation, however, do not appear to be necessary for NF-κB activation with smaller, therapeutic doses of IR (e.g., refs *4* and *5*). Indeed, IR inhibits proteasomal activities at doses as small as 0.2 Gy with maximal inhibition at 2 Gy (*4*, *6*). IKKβ has other functions, including phosphorylation of S536 in the transactivation domain of the p65 subunit (*7*−*10*). Serine 536 phosphorylation is independent of IκBα phosphorylation and important for enhancing p65 transactivation potential and modulating gene target selection.

Recent studies demonstrate that NO• and a metabolic derivative, peroxynitrite ($ONOO^-$), modulate NF-κB activity (*11*−*15*). For example, addition of a $ONOO^-$ donor to cultured cells stimulates NF-κB reporter activity without IκBα degradation (*11*). These findings and the evidence that a Ca^{2+}-dependent constitutive NO• synthase activity in epithelial cells is transiently stimulated by small IR doses (*16*−*19*) prompted the following investigation of NO• signaling in IR-induced activation of NF-κB.

MATERIALS AND METHODS

Cell Culture, Irradiation, and Transfection. CHO-K1 and MCF-7 cells were cultured and irradiated at a dose rate of 2 Gy/min with a ^{60}Co source as previously described (*18*). Cells were transfected with the LipofectAMINE PLUS kit (Invitrogen).

[†] Research was supported by National Institutes of Health Grants CA65896, CA72955, and CA89055 (R.B.M.) and HD39110 and HL070061 (S.M.B.) and an ASTRO Resident Research Grant (I.J.B.).

[‡] Data added to the Research Collaboratory for Structural Bioinformatics Protein Data Bank as entries 1IKN and 1NFI.

* To whom correspondence should be addressed: Department of Radiation Oncology, Massey Cancer Center, 401 College St., Richmond, VA 23298. Telephone: (804) 628-0857. Fax: (804) 828-6042. E-mail: rmikkels@vcu.edu.

[§] Department of Radiation Oncology, Massey Cancer Center, Virginia Commonwealth University.

[∥] Medical College of Georgia.

[⊥] Merck Research Laboratories.

[@] Department of Medicinal Chemistry, Virginia Commonwealth University.

[1] Abbreviations: NOS-1, constitutive NO• synthase; TNFα, tumor necrosis factor α; IKK, IκB kinase; IR, ionizing radiation; L-NNA, N^G-nitro-L-arginine; SD, standard deviation.

10.1021/bi701107z CCC: $37.00
Published on Web 10/02/2007

Reagents. The following primary antibodies were used: actin, nuclear lamin A/C, IκBα, NOS1, IKKβ, and p65 (Santa Cruz Biotechnology); nitrotyrosine (Upstate Biotechnology); and p50, phospho-S32/36-IκBα, and the 9E10 epitope of c-Myc (Cell Signaling).

Wild-type pCMV-IκBα from Clontech has two ATG start sites with the second having an optimal Kozak sequence. For this reason, an IκBα doublet was detected after SDS−polyacrylamide gel electrophoresis in early experimentation. Both proteins were, however, equally nitrated (e.g., Figures 2A,E and 4A). Amino acid substitution mutants were constructed from pairs of point mutation primers by PCR technology with wild-type pCMV-IκBα as the initial template. Mutations were verified by full-length sequencing. Another set of mutants was prepared with an N-terminal c-Myc epitope tag to facilitate analysis.

The luciferase-based reporter construct of NF-κB (pNF-κB-luc) was also purchased from Clontech. Luciferase activity was measured in cell lysates 24 h after IR exposure with a Luciferase Reporter Gene Assay Kit (Packard Bioscience) according to the manufacturer's directions.

The human shRNA IKKβ plasmid was provided by Upstate Biotechnology. The dominant negative NOS-1 mutant (HemeRedF) and its effects on expression and activity of NOS-1 in CHO and other cells have been described (*17*, *20*, *21*). Mouse NOS-1 siRNAs and All Stars Negative Control siRNA were purchased from QIAGEN. HiPerFect Transfection Reagent (QIAGEN) was used for transfection of CHO cells with siRNAs. Cells were seeded and transfected on the same day according to the manufacturer's reverse transfection protocol.

Measurement of Nuclear NF-κB DNA Binding Activity. CHO cells were seeded 48 h before radiation in 100 mm dishes and transfected the same day with the NOS1 siRNAs or 24 h later with a plasmid expressing the HemeRedF NOS-1 mutant. Incubation with 100 nM L-NNA was performed 4 h before radiation. NF-κB DNA binding activity in nuclear extracts prepared as described in ref *22* was measured with a NF-κB p65 ELISA kit (Stressgen Bioreagents) according to manufacturer's recommendations.

Biochemical Analyses. Immunoprecipitation and Western blotting methods have been described previously (*17*, *20*). Protein detection was by chemiluminescence with alkaline phosphatase-conjugated secondary antibodies or with secondary antibodies conjugated with infrared fluorescent dyes and imaging with the Odyssey Infrared Imaging System (Li-Cor Biosciences). Cellular NOS activity was measured with an arginine to citrulline assay as previously described (*17*, *20*).

Mass Spectrometry. All proteins were resolved by one-dimensional SDS−PAGE and silver stained. After being destained, proteins were in-gel digested with modified porcine trypsin (0.6 μg, Promega) alone or with *Streptomyces aureus* V8 protease (0.6 μg, Sigma Chemical Co.) for 12 h according to the method of Shevchenko (*23*). The resultant peptides were purified with Poros 20 R2 reverse phase packing (Applied Biosystems) and subjected to direct infusion nanospray using NanoES spray capillaries (PROXEON, Odense, Denmark) on an Applied Biosystems QSTAR pulsar XL mass spectrometer. MS spectra were collected in positive mode with an ion spray voltage of 800 V. Subsequent MS/MS spectra were collected and amino acid sequences obtained using BioAnalyst.

Structural Analysis. To determine the optimal geometry of nitrotyrosine, we performed quantum mechanical calculations using density functional theory with the 6-311+G(d,p) basis set, B3PW91 hybrid functionals, default spin configuration, and a net molecular charge of zero (*24*). Self-consistent field was calculated directly with a convergence limit of 2×10^{-5}. These parameters ensured that the optimized structure of nitrotyrosine was available for calculation of its various structural and chemical properties. The force constants for bonds, bond angles, and dihedrals were calculated using the Hessian matrix. Subsequently, charge distribution and electronic polarizability of nitro-tyrosine were calculated in a water solution to fully characterize the properties of this modified amino acid. These properties were properly entered in the CHARMM22 (*25*) parameter and topology files for use in NAMD2, a molecular dynamics algorithm (*26*, *27*). The validity of quantum mechanical calculations was established by ^{13}C NMR spectroscopy using commercially available 3-nitrotyrosine ethyl ester in D_2O (see the Supporting Information).

Two X-ray structures of the IκBα−NF-κB complex are found in the Protein Data Bank, 1NFI (2.7 Å resolution) (*28*) and 1IKN (2.3 Å resolution) (*29*). The *R* values for both structures were 0.223. The sequence enumerations are identical for IκBα and p65 but are shifted by three residues for the p50 subunit. The 1IKN structure was used for our analysis. Energy minimization was performed for 2500 steps, enabling energetic relaxation of the system.

For the HINT calculations, the PDB coordinates of control and nitrated IκBα−NF-κB complexes at the end of the minimization were used. We defined Y181 or nitro-Y181 as structure A and the remainder of the IκBα−NF-κB complex as structure B. The HINT program was then used to evaluate a comprehensive set of nonbonded interactions between structures A and B (hydrogen bonding, acid−base, hydrophobic−hydrophobic, acid−acid, base−base, and hydrophobic−polar) (*30*−*35*).

RESULTS

Inhibiting NOS-1 Blocks IR-Stimulated NF-κB Activity. Initial experiments tested whether radiation-induced NOS-1 activity contributed to an increase in NF-κB promoter activity measured with a luciferase-based reporter assay. CHO cells were cotransfected with the reporter plasmid and either an empty vector or the dominant negative mutant of NOS-1 (HemeRedF) whose expression was previously shown to inhibit IR-activated NOS activity in CHO cells (*17*, *20*). A single IR exposure of 5 Gy stimulated a 1.5−3-fold increase in NF-κB-dependent luciferase activity measured 24 h post-IR (e.g., Figures 1A,B,G and 2G). This increase in activity was similar to what others have observed with diverse cell types after an exposure to IR (*36*−*38*). Expression of HemeRedF completely inhibited IR-stimulated reporter gene expression and reduced basal reporter activity by 40−50% (Figure 1A). The effect of genetically inhibiting NOS-1 activity on NF-κB promoter activity was confirmed pharmacologically with the NOS inhibitor N^G-nitro-L-arginine (L-NNA). Incubating cells with L-NNA 4 h prior to irradiation significantly reduced both basal and IR-induced NF-κB promoter activity (Figures 1B,G and 2G).

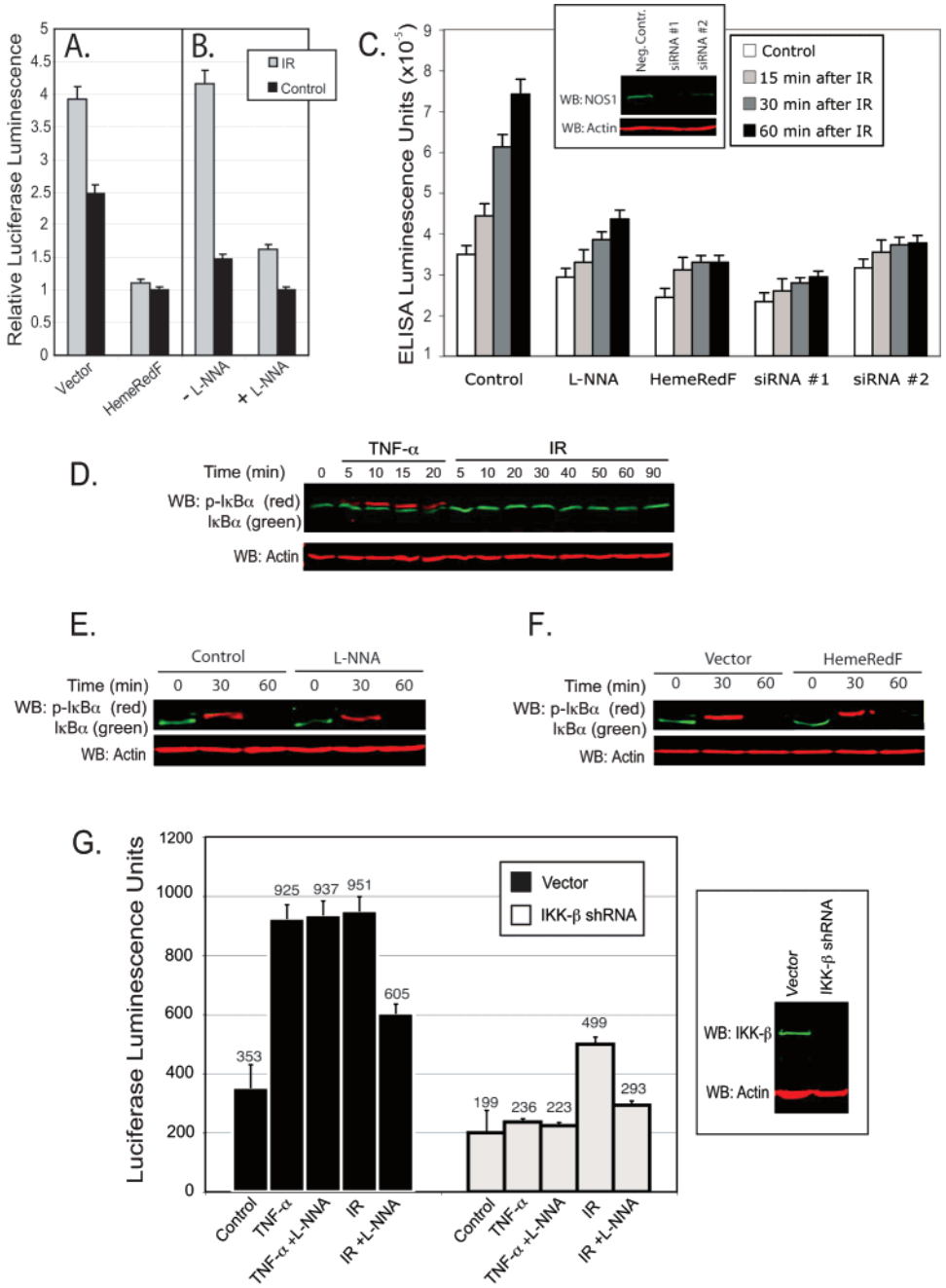

FIGURE 1: IR and TNFα activation of NF-κB. (A) CHO cells were cotransfected with pNF-κB-luc and either pHemeRedF (dominant negative mutant of NOS-1) or an empty vector as a control. Cells were irradiated (5 Gy) 48 h after transfection, and luciferase activity was measured in cell lysates 24 h later. (B) Forty-four hours after transfection with pNF-κB-luc, cells were treated with 100 nM L-NNA for 4 h prior to a 5 Gy IR exposure. Experimental data (for panels A and B) are presented as means ± SD for quadruplicate samples and are representative of experiments performed in triplicate. (C) CHO cells were seeded and transfected with NOS1 siRNAs on the same day or with HemeRedF plasmid 24 h later. Incubation with 100 nM L-NNA was performed 4 h before irradiation. Cells were irradiated (5 Gy) 48 h after seeding and harvested at the given time points after IR. Nuclear extracts of the cells were prepared and normalized relative to the total protein concentration. The ELISA was performed to measure specific DNA binding activity of NF-κB in the nuclear extracts. Experimental data are presented as means ± SD for triplicate samples. The embedded panel shows the level of NOS1 48 h after transfection with isRNAs. (D) MCF-7 cells were irradiated at 5 Gy and cell lysates analyzed by immunoblotting for phospho-S32/36-IκBα (red) and IκBα (green). As a positive control, cells were treated with 10 nM TNFα. Equal loading was verified by blotting with anti-actin (bottom panel). (E) Cells were pretreated with 100 nM L-NNA for 4 h prior to addition of 10 nM TNFα. Equal loading was verified by Western blotting of cell lysates with anti-actin (bottom panel). (F) MCF-7 cells were transfected with pHemeRedF or empty vector as a control. Cells were treated with TNFα (10 nM) 48 h after transfection. Equal loading was verified by immunoblotting cell lysates with anti-actin (bottom panel). (G) MCF-7 cells were cotransfected with pNF-κB-luc and either pIKK-β shRNA or the empty vector as a control. Cells were irradiated (5 Gy) or treated with TNFα 48 h after transfection, and luciferase activity was measured in cell lysates 24 h later. L-NNA (100 nM) was added to the cell cultures 4 h prior to IR exposure or TNFα treatment. Experimental data are presented as means ± SD for triplicate samples. The right panel shows Western blots of cell lysates validating the effectiveness of IKKβ shRNA treatment, 48 h after transfection. Cell lysates were probed with anti-IKKβ (green) and anti-actin antibody (red) as a loading control.

To further validate the role of NOS-1 in NF-κB activation by IR, cells were transfected with control and siRNA directed against NOS-1. The inset of Figure 1C demonstrates that both siRNAs that were tested were efficient in inhibiting

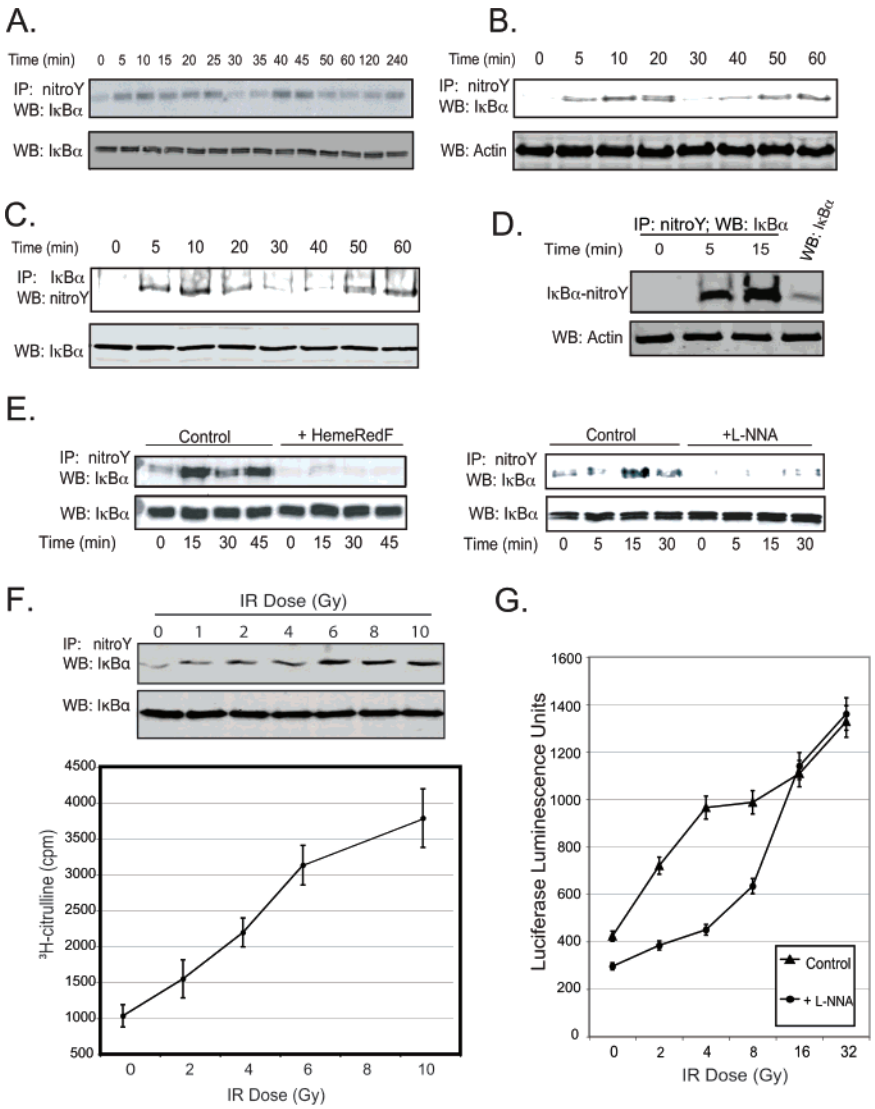

FIGURE 2: IR dose dependence of NOS-1 activity, NF-κB induction, and IκBα tyrosine nitration. (A) Tyrosine nitration of IκBα after IR (5 Gy) was monitored in CHO cells transfected with pCMV-IκBα-wild type and irradiated 48 h after transfection. Anti-nitrotyrosine immunoprecipitates were analyzed for IκBα by Western blotting. Equal loading was verified by immunoblotting cell lysates with anti-IκBα antibody (bottom panel). (B) Radiation-stimulated tyrosine nitration of endogenous IκBα in MCF-7 cells. MCF-7 cells were radiated (5 Gy), and cell lysate was prepared at the indicated time points. Anti-nitrotyrosine immunoprecipitates were analyzed with anti-IκBα antibody. For loading controls, equal amounts of each cell lysate were fractionated by electrophoresis and immunoblotted with anti-actin antibody. (C) MCF-7 cells were radiated as described for panel B. Anti-IκBα immunoprecipitates were probed with anti-nitrotyrosine antibody. For loading controls, equal amounts of each immunoprecipitate were fractionated by electrophoresis and blotted with anti-IκBα. (D) Whole-cell extracts from nontransfected cells were prepared 0 min (no IR) and 5 and 15 min post-IR (5 Gy). Anti-nitrotyrosine immunoprecipitates from total cell extracts were analyzed by immunoblotting with anti-IκBα and compared with 2% of total cellular IκBα (lane 4). Cell lysates were probed with anti-actin antibody as a loading control (bottom panel). (E) NOS activity modulates IκBα tyrosine nitration after IR (5 Gy). CHO cells were cotransfected with pIκBα and pHemeRedF or an empty vector. Alternatively, cells transfected with pIκBα were treated with 100 nM L-NNA 4 h prior to irradiation. The experimental protocol described for panel C was used to determine the effects of inhibiting NOS activity by HemeRedF expression or incubating cells with L-NNA (top panel). Bottom panels are loading controls of cell lysates probed with anti-IκBα antibody. (F) MCF-7 cells were lysed 15 min after being exposed to different IR doses. Anti-nitrotyrosine immunoprecipitates were analyzed by immunoblotting with anti-IκBα. Cell lysates were probed with anti-IκBα to verify equal loading (bottom panel). The graph shows results of the arginine−citrulline conversion assay with different doses of IR performed as previously described (*17*, *20*). Results are presented as the average of triplicate samples ± SD. (G) L-NNA inhibition of NF-κB activity after addition of different doses of IR. MCF-7 cells were transfected with pNF-κB-luc and irradiated 48 h after transfection. Luciferase activity was measured in cell lysates 24 h later. Cells were incubated with 100 nM L-NNA for 4 h prior to an IR exposure.

expression of NOS-1 in CHO cells. We compared the relative effects of siRNA transfection, expression of the NOS-1 mutant, HemeRedF, and the chemical inhibitor, L-NNA, with respect to their relative abilities to inhibit basal and IR-induced NF-κB. NF-κB activity for these analyses was measured using nuclear extracts in an ELISA for p65 binding to a NF-κB specific oligonucleotide consensus sequence. Results in Figure 1C show that all three methods of inhibiting NOS-1 activity were effective at blocking IR-stimulated NF-κB activity, although the molecular approaches appeared more effective. Further validation was obtained by following nuclear translocation of p65 subsequent to irradiation. As shown in Figure S3 of the Supporting Information, nuclear isolates were probed for p65 by Western blot analysis normalized with respect to nuclear lamin levels. The level of nuclear accumulation of p65 increased

within 10 min of irradiation by a mechanism inhibited by L-NNA.

Activation of NF-κB by a Small IR Dose Does Not Stimulate IκBα Phosphorylation. We tested whether small IR doses activated IKK measured as IκBα S32/36 phosphorylation and proteolysis. Via this assay, IKK activity was not stimulated at the IR doses that were used (≤5 Gy) (Figure 1D). Control experiments with TNFα stimulation showed enhanced but transient IκBα Ser32/36 phosphorylation and a progressive decrease in IκBα protein levels, indicating that this IKK-dependent activation mechanism was intact. Incubation with L-NNA or expression of HemeRedF did not inhibit IκBα S32/36 phosphorylation stimulated by TNFα (Figure 1E,F).

NF-κB activation by TNFα or IR at 5 Gy was also compared in cells transfected with shRNA specific to IKKβ to abrogate this activation pathway for NF-κB (Figure 1G). A cotransfected luciferase reporter construct was used to assess cellular NF-κB activity. Cells expressing shRNA exhibited IKKβ protein levels less than 10% of those of control cells, transfected with empty vector. This inhibition of IKKβ expression with shRNA reduced NF-κB basal activity by 50% and completely blocked stimulation by TNFα. In contrast to these observations with TNFα, IR-stimulated NF-κB activity was only reduced by approximately 50% with IKKβ shRNA expression. The remaining activity was inhibited by treatment with L-NNA (Figure 1G). Since both basal and IR-stimulated NF-κB activities were reduced by IKKβ shRNA expression, the fold activation with IR achieved in these cells was not significantly different from that of control, IKKβ-expressing cells.

Radiation Stimulates the Tyrosine Nitration of IκBα. IR activation of NOS stimulates $ONOO^-$ generation detected as tyrosine nitration of a number of proteins (*17*). We tested whether IR at 5 Gy stimulated the nitration of IκBα using CHO cells transfected with human wild-type IκBα. Anti-nitrotyrosine immunoprecipitates from lysates of control and irradiated cells were analyzed by the Western blot method for IκBα (Figure 2A). IR stimulated oscillating changes in IκBα tyrosine nitration with an initial maximum 10−20 min post-IR and a second maximum at ≈40 min. Similar results were obtained with endogenous IκBα in MCF-7 breast carcinoma cells (Figure 2B). The reciprocal experiment with immunoprecipitation of IκBα followed by blotting with anti-nitrotyrosine IgG showed the same oscillations in tyrosine nitration of IκBα without changes in IκBα protein expression levels (Figure 2C). Comparing amounts of endogenous tyrosine-nitrated IκBα with total IκBα suggests that up to 25% is transiently nitrated 15 min post-IR (Figure 2D). Basal and IR-induced tyrosine nitration of IκBα are both significantly inhibited by expression of HemeRedF or via incubation of cells with L-NNA (Figure 2E).

Previous studies demonstrated oscillations of NF-κB DNA binding that correlated with oscillations in total IκBα protein levels following TNFα treatment of cells (*39*, *40*). This work with small doses of IR, in contrast, showed no measurable change in total cellular IκBα levels after IR at 5 Gy (Figure 2A,C,E). Thus, it is unlikely that selective proteolysis of nitrated IκBα accounts for the observed oscillations in IκBα nitration following an IR exposure. Proteolytic degradation of IκBα is not a requirement for NF-κB activation (e.g., refs *11* and *41*). Furthermore, IR inhibits proteasome activities (*4*, *6*).

Radiation Dose−Response Analyses Comparing Cellular NOS Activity, IκBα Tyrosine Nitration, and NF-κB Transcription Reporter Activity. Our previous studies (*17*, *18*) using a fluorescent dye to measure the levels of reactive oxygen and nitrogen species demonstrated a dose response which saturated at doses of >6 Gy. These findings were confirmed by measuring as a function of IR dose cellular NOS activity directly with an arginine−citrulline conversion assay or indirectly by assessing tyrosine nitration of IκBα (Figure 2F). Both measures of $NO^\bullet$ activity progressively increased with IR dose and reached relative plateaus at doses greater than 6 Gy. A similar dose−response curve was observed for NF-κB reporter activity (Figure 2G). At IR doses above 8 Gy, L-NNA was a less effective inhibitor of NF-κB activation. At ≥16 Gy, inhibition of NOS-1 activity with L-NNA had no effect on IR-induced NF-κB activity.

Tyrosines 181 and 305 of IκBα Are Nitrated after Irradiation of Intact Cells. A genetic approach was also used to determine sites of nitration. Each tyrosine of IκBα was individually mutated to phenylalanine. CHO cells were transfected with plasmids expressing all eight Myc-tagged Y-to-F mutants and Myc-tagged wild-type IκBα. Tyrosine nitration of the mutants and wild type was assessed as a function of time following an IR exposure of 5 Gy by immunoaffinity purification of the nitrated proteins followed by Western blot detection with anti-Myc (Figure 3). To facilitate comparisons between blots, each blot included one lane of wild-type Myc-tagged IκBα obtained from cell lysates nitrated with 50 μM $ONOO^-$ and subsequently immunopurified with anti-nitrotyrosine-conjugated agarose beads. All single mutants demonstrated with approximately identical frequencies oscillating levels of nitrated IκBα following irradiation. However, for the Y181F and Y305F single mutants, the amplitude in IR-induced nitration was significantly lower than that observed for the wild type and the other tyrosine mutants. A double mutant (Y181F/Y305F) was constructed to test whether these two tyrosines were exclusively nitrated following irradiation. As shown in the bottom panels of Figure 3, the double mutant was not nitrated after being exposed to 5 Gy radiation dose.

Peroxynitrite Treatment of the NF-κB−IκBα Complex Nitrates Tyrosines 181 and 305 of IκBα and Dissociates the IκBα−NF-κB Complex. Initial experiments using the different IκBα mutants and treatment of cell lysates with $ONOO^-$ also demonstrated a high degree of specificity in the $ONOO^-$-induced nitration of IκBα. As observed with radiation, only mutant proteins for tyrosines 181 and 305 showed significantly reduced levels of nitration following addition of a single bolus of $ONOO^-$. The double mutant for these two tyrosines was not nitrated at all (Figure 4A,B).

We attempted to validate the genetic evidence for $ONOO^-$-induced nitration of these two tyrosines by mass spectrometry. The cell lysate with overexpressed IκBα was nitrated with $ONOO^-$ and nitrated IκBα isolated by precipitation with anti-nitrotyrosine IgG, resolved by gel electrophoresis, and processed for mass spectroscopy. After proteolysis, five IκBα peptides were identified for coverage of 21%, and this included four of the eight tyrosines of IκBα (Table S1 of the Supporting Information). The tryptic peptide containing tyrosine 181 is more than 40 amino acids long and was not

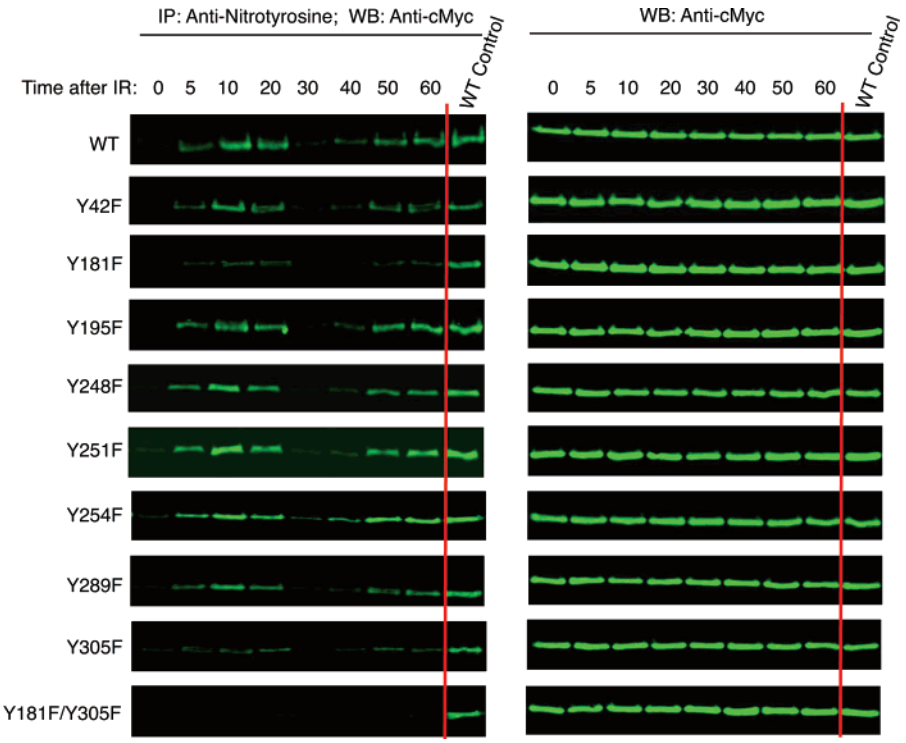

FIGURE 3: Site-directed mutagenesis and identification of IκBα tyrosines nitrated after irradiation. CHO cells were transfected with wild-type c-Myc-tagged IκBα, different Y → F mutants, and the Y181F/Y305F double mutant and irradiated with 5 Gy 48 h after transfection. Cells were lysed at the certain time points after IR. Anti-nitrotyrosine immunoprecipitates were analyzed by immunoblotting with anti-c-Myc (left panels). Cell lysates were probed with anti-c-Myc to verify equal loading of c-Myc-tagged IκBα (right panels). As a positive control and to facilitate comparisons, c-Myc-tagged IκBα in cell lysates of overexpressing cells was nitrated with 50 μM $ONOO^-$. The nitrated IκBα was immunopurified as described and run on each blot (the last line of each panel).

detected in the mass spectra. Attempts with different peptide cutting agents to obtain an identifiable peptide containing tyrosine 181 proved to be unsuccessful. However, a 20-amino acid peptide of IκBα (amino acids 295−314) was sequenced and identified in the un-nitrated form and also as a peptide with a mass consistent with tyrosine nitration (+45 Da; Figures S1 and S2 of the Supporting Information). Our initial attempts to sequence the only tyrosine in this peptide, Y305, to confirm its nitration, have not been successful. Additional mass spectroscopic analysis of the IκBα 295−314 peptide indicated that C308 was modified by propionamide (an acrylamide adduct), indicating that C308 was not oxidized by the $ONOO^-$ treatment. Methionine 91 in peptide 88−95 was also not oxidized. Both findings support the conclusion that a bolus $ONOO^-$ treatment is relatively specific in its effects on amino acid modification of IκBα (*42*, *43*).

We tested whether in vitro nitration with exogenous $ONOO^-$ dissociated the IκBα−NF-κB complex. A single bolus addition of $ONOO^-$ was used since the short half-life of $ONOO^-$ (<1 s) enhances specificity in its reactions (e.g., refs *42* and *43*). Cell lysates prepared under mild nondenaturing conditions were treated with 200 or 400 μM $ONOO^-$. Two consecutive immunoprecipitations were performed. Agarose-conjugated anti-p65 IgG was used to pull down the NF-κB−IκBα and free NF-κB complexes. After centrifugation to remove these complexes, the resulting supernatants were incubated with agarose-conjugated anti-IκBα IgG to pull down free IκBα. Western blots of the immunoprecipitates were probed with antibodies against p65, IκBα, and nitrotyrosine. With increasing concentrations of $ONOO^-$, a decreasing amount of IκBα was associated with p65 with a corresponding increase in the amount of free tyrosine-nitrated IκBα (Figure 4C). Tyrosine-nitrated IκBα did not co-immunoprecipitate with NF-κB (lanes 5 and 6). For long exposure times and at high $ONOO^-$ concentrations, a broad smear of nitrotyrosine staining was observed in p65 immunoprecipitates but with no distinct band for IκBα (lane 3). Neither p50 nor p65 was nitrated under these conditions (data not shown), and the p50−p65 dimer remained intact as shown by co-immunoprecipitation (Figure 4D). These results suggest that tyrosine nitration of IκBα dissociates the NF-κB−IκBα complex, releasing the p50−p65 dimer.

Cell lysates were prepared from cells transfected with Myc-tagged wild-type IκBα and mutants (Y42F, Y181F, and Y305F) and treated with 200 μM $ONOO^-$. NF-κB immunoprecipitates obtained with anti-p65 were probed for p65 and Myc-tagged IκBα. $ONOO^-$ treatment decreases the amount of IκBα associated with p65 in the wild type and all mutants tested except for the Y181F mutant (Figure 4E). These results suggest that Y181 is critical to the stability of the NF-κB−IκBα complex following $ONOO^-$ treatment.

CHO cells were cotransfected with the NF-κB reporter gene and either the Myc-tagged wild type or the Myc-tagged IκBα Y-to-F mutants. As expected, overexpression of the wild type or mutants inhibited basal NF-κB reporter activity (≈90%). However, a significant IR-induced activation (∼1.4) was still observed in cells expressing the wild type or the Y42F and Y305F mutants (Figure 4F). This is observed if promoter activity is expressed in terms of absolute values or as ratios of reporter activities of irradiated to control cells. In contrast, IR-stimulated NF-κB reporter activity was completely blocked in cells expressing the Y181F mutant, demonstrating an important role for Y181 in the mechanism of IR-induced activation of NF-κB. Basal NF-κB activity of

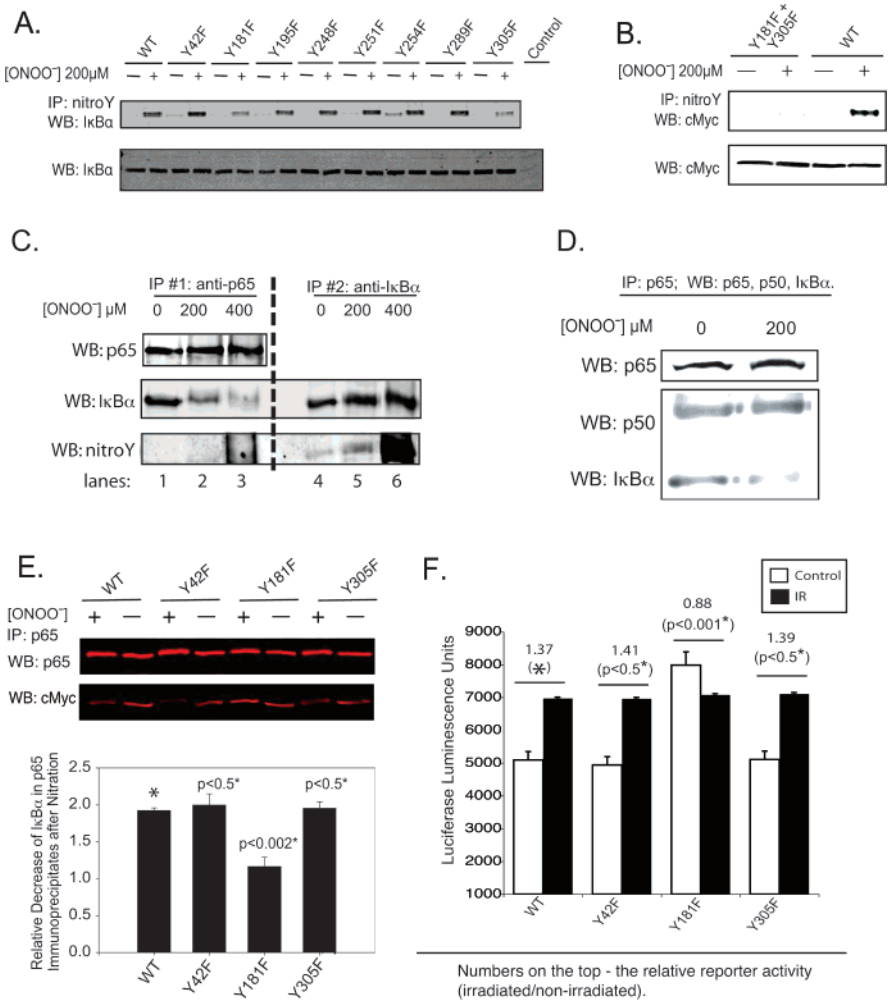

FIGURE 4: Tyrosine nitration of IκBα dissociates the IκBα−NF-κB complex. (A) Cell lysates from CHO cells expressing wild-type IκBα and different Y → F mutants were treated with $ONOO^-$. Anti-nitrotyrosine immunoprecipitates were analyzed by immunoblotting with anti-IκBα. Cell lysates were probed with anti-IκBα to verify equal loading (bottom panel). The control was the untransfected sample. (B) Cell lysates from CHO cells expressing wild-type c-Myc-tagged IκBα and the Y181F/Y305F double mutant were treated with $ONOO^-$. Anti-nitrotyrosine immunoprecipitates were analyzed by immunoblotting with anti-c-Myc. Cell lysates were probed with anti-c-Myc to verify equal loading of c-Myc-tagged IκBα (bottom panel). (C) p65 and IκBα immunoprecipitates were obtained from $ONOO^-$-treated cell lysates as described in the text. Preliminary control experiments demonstrated that the amount of antibody used was sufficient to fully immunoprecipitate the target antigen. Samples from the first (lanes 1−3) and second (lanes 4−6) immunoprecipitations were analyzed for p65 (top panel) and IκBα (middle panel) by immunoblotting. The blots were probed simultaneously with anti-nitrotyrosine antibody (bottom panel). (D) After $ONOO^-$ treatment, anti-p65 immunoprecipitates were analyzed for p50 and IκBα. The loading control was p65 (top panel). (E) CHO cells were transfected with plasmids encoding the c-Myc-tagged wild type and the Y → F mutants of IκBα. Cell lysates prepared 24 h after transfection were treated with 200 μM $ONOO^-$. Anti-p65 immunoprecipitates were analyzed by Western blotting for p65 and c-Myc. The fluorogram from one of two experiments is shown. The fluorescence intensity readings from two different experiments were used to calculate the relative nitration-induced decrease in the level of IκBα associated with p65 calculated as the average intensity of IκBα normalized to the loading control (p65 intensity) ± SD. The *p* values were determined by Student's *t* test relative to wild type transfected cells (asterisks). (F) DNA binding activity of NF-κB was estimated as described in the legend of Figure 1 after cotransfection of pNF-κB-luc with wild-type IκBα and the indicated Y → F mutants. The increase in activity after IR was normalized relative to that of cells cotransfected with pNF-κB-luc and empty vector. Data are means ± SD for quadruplicate samples and representative of experiments performed in triplicate. The *p* values were determined by Student's *t* test relative to the wild-type transfected cells (asterisks).

Y181F IκBα-mutant expressing cells was moderately higher relative to the basal NF-κB activity of cells overexpressing the wild type or the other IκBα mutants (Figure 4F). This is consistent with a previous analysis of different IκBα mutants showing that a Y181A mutant had a slightly lower affinity for the p50−p65 heterodimer (*44*). The variability in basal activity (e.g., Figure 5A) probably reflects a difference in expression levels.

Tyrosine 42 was also examined because previous reports indicated that its phosphorylation was important for oxidative activation of NF-κB without degradation of IκBα (*41*, *45*). However, mutation of Y42 to phenylalanine had no effect on either the stability of the NF-κB−IκBα complex after $ONOO^-$ treatment (Figure 4E) or IR-induced NF-κB promoter activity (Figure 4F).

Mutation of Tyrosine 181 Blocks IR- but Not TNFα-Induced NF-κB Activity. The effects of overexpressing wild-type IκBα or the Y181F and S32A/S36A mutants of IκBα on IR- and TNFα-stimulated NF-κB activities were compared in MCF-7 cells. Serines 32 and 36 are phosphorylated by an IKK-dependent mechanism, and thus, the double mutant at these sites is a super-repressor for those activation mechanisms that proceed solely through IKK (*1*, *39*). MCF-7 cells demonstrate a relatively weak NF-κB response to TNFα

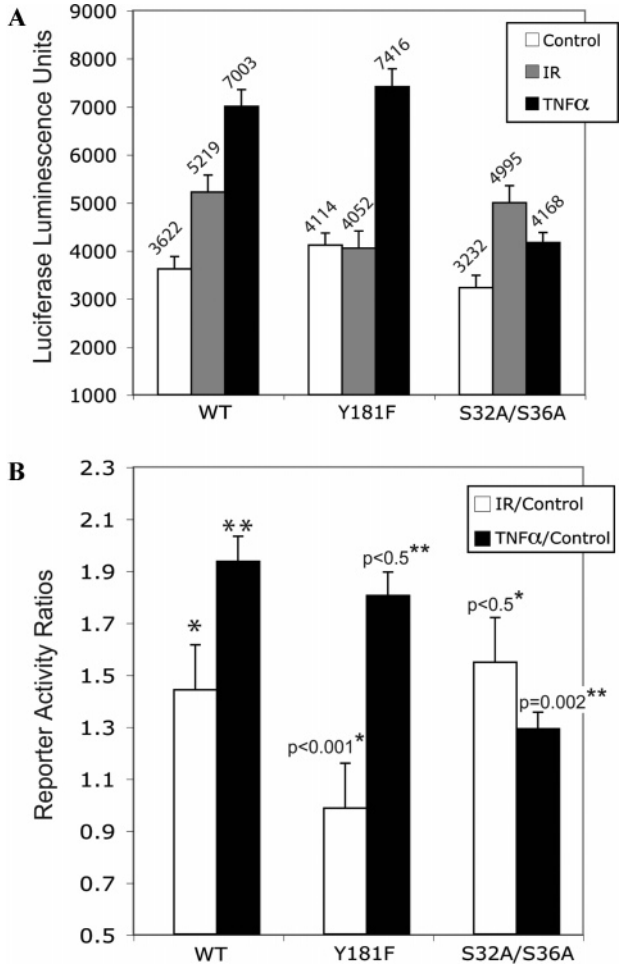

FIGURE 5: IκBα Y181F can play the role of supermutant in the radiation-dependent NFκB activation. (A) MCF-7 cells were cotransfected by pNF-κB-luc with wild-type IκBα, Y181F mutant IκBα, or S32A/S36A mutant IκBα. Cells were irradiated (5 Gy) or incubated with TNFα (10 nM) 48 h after transfection, and luciferase activity was measured in cell lysates 24 h later. (B) Absolute luminescence values are provided in panel A, converted into reporter activity ratios of treated vs nontreated cells. Data are means ± SD for quadruplicate samples and representative of experiments performed in triplicate. The *p* values (one asterisk) were determined by Student's *t* test relative to the wild-type IκBα-transfected cells for radiated-to-nonradiated ratios. The *p* values (two asterisks) were determined by Student's *t* test relative to the wild-type IκBα-transfected cells for TNFα-treated-to-nontreated ratios.

compared to other cell types, reflecting the variable amount of TNFα receptor in these cells (*46*). Nonetheless, the results in Figures 1G and 5 demonstrate that as with other cell types, the TNFα response proceeds through a mechanism involving IKK and serines 32 and 36. The experimental results are presented in absolute amounts of reporter luciferase activity (Figure 5A) or as ratios of treated versus control activities (Figure 5B). Expression of the S32A/S36A double mutant was significantly more effective than that of wild-type IκBα in suppressing TNFα-stimulated NF-κB activity. The Y181F mutant and wild-type IκBα, in contrast, were no different in their effectiveness as inhibitors of TNFα-stimulated NF-κB activity. Different results were obtained with IR as the activating mechanism. The Y181F mutant was significantly more effective at suppressing IR-induced NF-κB activity but was without any super-repressor activity with TNFα as the inducing agent. The results with the S32A/S36A mutant and IR parallel the findings provided above demonstrating that IR at the doses used here did not stimulate IκBα phosphorylation and degradation and that blocking expression of IKK with shRNA only partially inhibited IR-stimulated NF-κB activation (Figure 1G).

A Structural Analysis of the Effects of Y181 Nitration on the IκBα−NF-κB Complex. The experimental results with IR and exogenous $ONOO^-$ coupled with the site-directed mutagenesis studies strongly support a mechanism of Y181 nitration in NF-κB activation by IR. Other oxidative modifications of IκBα and nitration of either p50 or p65 after IR or $ONOO^-$ treatments were not detected. To further substantiate a role for Y181 nitration in IR-induced dissociation of the IκBα−NF-κB complex, an assessment of hydropathic interactions of Y181 with neighboring residues was made and molecular dynamics simulations were performed.

A computational chemistry program HINT (hydropathic interactions) permits the quantitative analysis of all possible noncovalent atom−atom interactions, including hydrogen bonding, Coulombic, acid−base, and hydrophobic interactions, using the crystal structure of proteins (*47*−*49*). HINT uses empirically derived constants based on thermodynamic hydropathy values from solvent partition measurements. The more positive the HINT value, the more energetically favorable the change in free energy. HINT calculations have accurately estimated changes in free energy resulting from site-specific mutations and their effect on hemoglobin dimer−tetramer assembly (*48*, *49*). Using HINT calculations, the interactions of Y181 or nitro-Y181 with the remainder of the NF-κB−IκBα complex were compared on an atom-by-atom basis with an 8 Å cutoff.

The initial calculations required a quantum-mechanical comparison of the unmodified tyrosine residue with the nitrated form to generate topology files for tyrosine and nitrotyrosine (Figure S4 of the Supporting Information). These calculations demonstrated an altered side chain electron distribution that accounts for the measured decrease in the p*K* of the phenolic group from ~10 to ~7 (*50*, *51*). The portion of nitrotyrosine containing the NO_2 group was highly electronegative with the most electropositive portion localized over the C_α and C_β atoms. This results in a dipole moment vector oriented almost parallel with the $C_\epsilon-NO_2$ bond (Figure S4 of the Supporting Information). The magnitude of the calculated dipole moment of nitrotyrosine was 5.78 D, compared with 3.63 D for tyrosine. Without nitration, the tyrosine dipole moment vector was oriented along the long axis of the side chain aligning the hydroxyl group of the phenol ring with the C_β and C_α atoms.

Crystallographic studies of the NF-κB−IκBα complex show that IκBα is oriented so that fingers 3/4, 4/5, and 5/6 of IκBα contact the p50 subunit (*28*, *29*). Y181 and N182 extending from finger 3/4 have multiple contacts with p50. Y181, in particular, has an important role in these interactions since it forms hydrogen bonds with p50 K252 and R258, π-stacks with Y351, and makes multiple van der Waals contacts with A260, P327, and L349. Table 1 shows results on an atom-by-atom basis of HINT calculations using a cutoff distance between atoms of 8 Å. "Nitration" of Y181 using the generated topology file described above causes significant destabilizing changes in these interactions as seen by the net negative increase in the total HINT score. A more instructive presentation of the HINT scores is shown in the

Table 1: HINT Score Calculations (Y181 before and after nitration with p50 and IκBα)

Before Nitration

	Residue	Residue Atom	nitroTyr Atom	Interaction Score	Interaction Type
NFκB (p50)	ARG258	NH2	CA	-15	Hydroph./Polar
	ARG258	NH2	CB	-54	Hydroph./Polar
	ALA260	CB	CA	29	Hydrophobic
	ALA260	CB	CB	34	Hydrophobic
	ALA260	CB	CD2	12	Hydrophobic
	PRO327	CD	OH	-23	Hydroph./Polar
	PRO327	CB	OH	-34	Hydroph./Polar
	PRO327	CG	OH	-122	Hydroph./Polar
	LEU349	CD1	OH	-49	Hydroph./Polar
	LEU349	CD1	CD2	13	Hydrophobic
	LEU349	CD1	CE2	19	Hydrophobic
	TYR351	CB	OH	-45	Hydroph./Polar
	PRO352	CD	OH	-17	Hydroph./Polar
IκBα	ARG140	CB	OH	-14	Hydroph./Polar
	ARG140	NH1	OH	-15	Acid/Acid
	ARG140	NH1	CD2	13	Acid/Base
	ARG140	NH1	CE2	21	Acid/Base
	ASP141	O	OH	-15	Base/Base
	PHE142	O	CD1	-15	Hydroph./Polar
	PHE142	O	CE1	-15	Hydroph./Polar
	ARG143	O	CA	-15	Hydroph./Polar
	ARG143	O	CB	-28	Hydroph./Polar
	ARG143	O	CD1	-14	Hydroph./Polar
	GLY144	CA	CE1	13	Hydrophobic
	GLY144	CA	OH	-44	Hydroph./Polar
	GLY144	CA	CD2	11	Hydrophobic
	GLY144	CA	CE2	15	Hydrophobic
	ASN180	OD1	CA	-20	Hydroph./Polar
	ASN180	O	CA	-82	Hydroph./Polar
	ASN180	O	CB	-19	Hydroph./Polar
	ASN182	NI	CA	-350	Hydroph./Polar
	ASN182	NI	CB	-69	Hydroph./Polar
	ASN182	OD1	CA	-12	Hydroph./Polar
	ASN182	OD1	CB	-14	Hydroph./Polar
	GLY183	N	CA	-13	Hydroph./Polar
			Total HINT Score	-904.132	

After Nitration

Residue	Residue Atom	nitroTyr Atom	Interaction Score	Interaction Type
PRO327	CD	OH	-23	Hydroph./Polar
PRO327	CD	ON1	-16	Hydroph./Polar
PRO327	CD	ON2	-50	Hydroph./Polar
PRO327	CB	OH	-33	Hydroph./Polar
PRO327	CB	NE2	31	Hydrophobic
PRO327	CB	ON1	-77	Hydroph./Polar
PRO327	CB	ON2	-106	Hydroph./Polar
PRO327	CG	OH	-119	Hydroph./Polar
PRO327	CG	NE2	57	Hydrophobic
PRO327	CG	ON1	-93	Hydroph./Polar
PRO327	CG	ON2	-424	Hydroph./Polar
LEU349	CB	ON1	-33	Hydroph./Polar
LEU349	CG	ON1	-15	Hydroph./Polar
LEU349	CD1	OH	-47	Hydroph./Polar
LEU349	CD1	CD2	14	Hydrophobic
LEU349	CD1	NE2	142	Hydrophobic
LEU349	CD1	ON1	-853	Hydroph./Polar
LEU349	CD1	ON2	-158	Hydroph./Polar
LEU349	CD2	NE2	23	Hydrophobic
LEU349	CD2	ON1	-190	Hydroph./Polar
ARG140	NH1	NE2	228	Hydrogen Bond
ARG140	NH1	ON1	995	Hydrogen Bond
ARG140	NH1	ON2	261	Hydrogen Bond
ARG140	NH2	NE2	16	Acid/Base
ARG140	NH2	ON1	113	Acid/Base
ARG140	NH2	ON2	31	Acid/Base
ASP141	O	OH	-12	Base/Base
PHE142	O	CD1	-15	Hydroph./Polar
PHE142	O	CE1	-15	Hydroph./Polar
ARG143	O	CA	-15	Hydroph./Polar
ARG143	O	CB	-28	Hydroph./Polar
ARG143	O	CD1	-14	Hydroph./Polar
GLY144	CA	CE1	13	Hydrophobic
GLY144	CA	OH	-41	Hydroph./Polar
GLY144	CA	CD2	12	Hydrophobic
GLY144	CA	NE2	32	Hydrophobic
GLY144	CA	ON1	-40	Hydroph./Polar
GLY144	CA	ON2	-34	Hydroph./Polar
GLY144	O	NE2	-33	Base/Base
GLY144	O	ON1	-76	Base/Base
GLY144	O	ON2	-48	Base/Base
THR179	O	NE2	-21	Base/Base
THR179	O	ON1	-157	Base/Base
THR179	O	ON2	-20	Base/Base
ASN182	NI	CA	-350	Hydroph./Polar
ASN182	NI	CB	-69	Hydroph./Polar
		Total HINT Score	-1783	

Summary of HINT Scores - IκBα Y181 with:

	Before Nitration	After Nitration
p50	-218	-1970
IκBα	-686	+187

summary inset of Table 1, where the total HINT scores for interactions of IκBα Y181 with p50 and with other residues of IκBα are separated. Nitration results in a significant destabilization of p50−IκBα interactions as indicated by a net negative increase in the HINT score from −218 to −1970. Assuming approximately 1 kcal/mol per 500 HINT, this represents a change in free energy of approximately 3 kcal/mol. In contrast, the nitration-induced change in HINT scores for interactions of Y181 with other IκBα residues within 8 Å is consistent with a net stabilizing effect. Major contributions to this positive interaction are the acid/base and hydrogen bond interactions of the nitro group with R140 of IκBα (Table 1 and Figure 6A).

To experimentally test for this, the R140A IκBα mutant was constructed, and the relative affinities of wild-type and R140A Myc-tagged IκBα for NF-κB were compared by co-immunoprecipitation with the anti-p65 antibody (Figure 6B). The affinity of the R140A mutant for NF-κB is considerably reduced relative to that of the wild type even in the absence of nitration. These results do not allow for any statement about the role of this particular interaction in the effect nitration on the stability of the IκBα−NF-κB complex. However, they underline the importance of this surface area of IκBα in its interactions with the p50−p65 heterodimer and the potential for their disruption by tyrosine nitration.

DISCUSSION

The experimentation described above indicates a new mechanism for NF-κB activation. IR is shown to stimulate NF-κB activity by a mechanism in which IκBα Y181 is nitrated as a consequence of NOS-1 activation, leading to dissociation of intact IκBα from NF-κB. Hence, this mechanism of NF-κB activation does not depend on IKK-dependent phosphorylation and proteolytic degradation of IκBα. Modeling of free energy changes is consistent with the experimental findings that IR-induced Y181 nitration disrupts the noncovalent interactions of Y181 with p50, dissociating the IκBα−NF-κB complex. The apparent lack of IκBα degradation following treatment of cells with small IR doses is also in accord with findings that IR at doses of >0.2 Gy significantly inhibits proteosome activities (*4*, *6*). The IR dose−response analysis demonstrates a progressive increase in the level of NF-κB activation up to the largest dose tested, 32 Gy. However, only at IR doses below 8 Gy is substantial inhibition observed with the NOS inhibitor L-NNA. Similar dose responses are observed for IR-induced IκBα nitration and NOS-1 activation.

The experimental results suggest that NF-κB is activated by IR through both IKKβ-independent and IKKβ-dependent mechanisms. The IKKβ-independent pathway involving tyrosine nitration of IκBα is prominent at IR doses of ≤8 Gy, whereas the IKKβ-dependent pathway involving IκBα phosphorylation and/or proteolysis becomes more prominent at IR doses of >8 Gy. Dose-dependent mechanisms are also indicated in the IKKβ knockdown experiments. Whereas shRNA treatment completely abrogates TNFα-induced NF-κB activity, it only partially decreases IR-induced activity. The remaining activity is inhibited by NOS inhibitor L-NNA.

Analysis of the kinetics of NF-κB activation following small- or large-dose IR is also indicative of different mechanisms. A previous study using electrophoretic mobility shift analysis monitored activation of NF-κB in HeLa cells

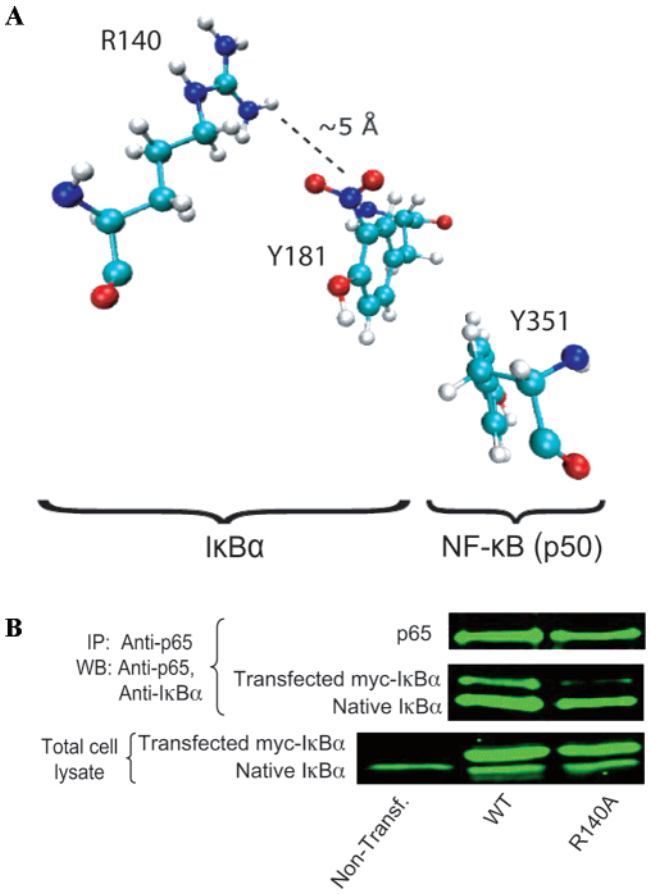

FIGURE 6: Spatial relationship between the NO_2 group of Y181 and R140 of IκBα. (A) R140, an inherently electropositive residue, buffers the electronegative charge of nitrated Y181 via long-range electrostatic interactions as evidenced by out-of-plane rotation of the NO_2 group. The optimized structure of nitrated tyrosine indicates that the most optimal structure exists when the NO_2 group is in the plane of the phenol ring. (B) R140 of IκBα is responsible for the stability of the NF-κB−IκBα complex. CHO cells were transfected with wild-type and R140A mutant Myc-tagged IκBα. Cell lysates were prepared 24 h after transfection and immunoprecipitated by anti-p65 antibodies. Immunoprecipitates were analyzed by blotting with anti-p65 and anti-IκBα antibodies. Equal amounts of cell lysates were used as a transfection control (bottom panel).

after 20 Gy (*52*). No activation was observed at 30 min, a slight increase at 1 h, and maximal activation at 2 h. This contrasts with the responses obtained within minutes of exposure to smaller doses of IR (Figures 1C and 2) or to TNFα (*39*). IR-stimulated nitration of IκBα is observed 5 min post-irradiation at 5 Gy, the earliest time point tested (Figure 2). In contrast, phosphorylation of IκBα Ser-32 or -36 is first observed 45 min post-irradiation with 20 Gy (*39*).

The IKKβ-dependent and -independent pathways are not mutually exclusive. This is suggested by the partial inhibition of NF-κB signaling at the smaller doses of IR by shRNA knockdown of IKKβ. However, the IKKβ mechanisms may differ depending on IR dose. For example, different mechanisms may reflect the cellular localization of the oxidative/nitrosative events: DNA damage in the nucleus and oxidative/nitrosative events in the cytoplasm. Further experiments are necessary to test this hypothesis. IKKβ can also modulate NF-κB transcriptional activity in the cytoplasm through an IκBα-independent mechanism: phosphorylation of the p65 subunit in its transactivation domain at S536 (*7*−*10*).

NF-κB activation by reactive nitrogen species has been previously investigated using a $ONOO^-$ donor, SIN-1 (*11*). NF-κB activity measured with a luciferase-based reporter assay was stimulated by a mechanism not blocked by the proteosome inhibitor, MG132, nor was IκBα degradation associated with the stimulation. These experimental findings directly relate to the results reported here with IR. Thus, our results provide a mechanism for how SIN-1 and other cellular $ONOO^-$-generating processes can activate NF-κB signaling.

A previous analysis of several IκBα mutants demonstrated that the Y181A mutation was most defective for formation of a complex with NF-κB (*44*). However, all IκBα mutants that were examined, including Y181A, still bound NF-κB with nanomolar affinities, suggesting that several binding elements contribute to the overall stability of the NF-κB−IκBα complex. This conclusion would appear to be in conflict with the findings presented here that mutation of Y181 alone completely blocks IR-stimulated NF-κB DNA binding activity and $ONOO^-$-induced disruption of the NF-κB−IκBα complex. A likely explanation is that nitration of tyrosine is a much more disruptive protein modification than substitution of an alanine for tyrosine. Besides introducing a bulky substituent, tyrosine nitration significantly alters the dipole moment of tyrosine and reduces the phenolic p*K* by 2−3 units, effectively introducing a net negative charge into a relatively nonpolar restricted space. Other studies have demonstrated that nitration of a specific tyrosine in proteins can have significant structural and functional consequences for proteins (e.g., refs *53*−*57*). It is also important to note that the studies by Huxford et al. (*44*) used a bacterial expression system with a truncated IκBα lacking both N- and C-terminal elements, including Y305. Nitration of Y305 may have an important role in modulating the stability of the NF-κB−IκBα complex.

Tyrosine 305 of IκBα is also nitrated following irradiation or an acute $ONOO^-$ treatment. We were unable to model the effects of Y305 nitration on the stability of the IκBα−NF-κB complex because both available crystal structures of the IκBα−NF-κB complex lack the C-terminal regions containing Y305. From the 1IKN structure, it is clear that a turn in secondary structure occurs around P215 and the C-terminal portion of IκBα wraps on itself and runs along the interface with p65 and p50 subunits of NF-κB. Tyrosine 305 is part of this C-terminal sequence, and its nitration can presumably contribute to disruption of noncovalent interactions stabilizing the IκBα−NF-κB complex. Is Y181 and Y305 nitration cooperative, and is nitration of both residues required for rapid dissociation of the complex? Judging from the results of our work, it appears that nitration of Y181 is alone sufficient to destabilize the signaling complex, but the kinetics of dissociation of IκBα from NF-κB may be affected by additional nitration of Y305. A previous report also provides evidence that phosphorylation of Y305 increased the in vivo stability of IκBα (*58*). It is possible that its nitration serves a similar purpose. Some investigations have suggested that nitrotyrosine may mimic phosphotyrosine binding sites (e.g., ref *59*). Further experimentation will be necessary to test these mechanisms involving Y305.

Experiments described here and in other published work demonstrate a high degree of selectivity in what tyrosines are nitrated by an acute $ONOO^-$ treatment (*60*). If complexed with the p50−p65 heterodimer, IκBα is nitrated on only two

of eight tyrosines following an IR exposure of intact cells or treatment of cell lysates with $ONOO^-$. Under the same in vitro conditions, attempts to nitrate purified IκBα with $ONOO^-$ have proven to be unsuccessful (C. S. Rabender, unpublished data). This suggests that the tertiary or quaternary structures of IκBα are important in determing its susceptibility to nitration by $ONOO^-$. An analysis of nitrated proteins suggests that no specific structural feature alone determines nitration (*60*, *61*). Tyrosines located in loop structures have an increased probability for nitration (*60*, *61*), and Y181 is located in the β-turn loop between the third and fourth ankyrin repeats.

No amino acid consensus sequence has been identified, although it has been suggested that nitrated tyrosines are generally but not always near acidic amino acid residues (*60*). This is true for Y305 with one glutamate in the proximity (KPFLY^{305}EIK), but this is not the case for Y181 (KATNY^{181}-NGHT). There are also no acidic amino acids from p50 or p65 at the interface near Y181 of IκBα that can contribute to this possible electrostatic environment. A more recent report on endogenously nitrated proteins of the brain argues for the importance of a positively charged amino acid near sites of nitration (*61*). This criterion is fulfilled by both Y181 and Y305 of IκBα.

The short half-life of $ONOO^-$ predicts that the proximity of the protein to the $ONOO^-$ source is also important in selectivity (*19*, *60*). The primary source of IR-stimulated cellular $ONOO^-$ is the mitochondrion, either by activity of a mitochondrial NOS-1 isoform or as a consequence of respiration-generated superoxide anion that reacts with relatively stable $NO^\bullet$ produced elsewhere in the cell (*16*, *19*, *60*, *62*). A reversible mitochondrial protein tyrosine nitration initiated by hypoxia/reoxygenation has been described (*62*), and there are reports of mitochondrial localization of the IκBα−NF-κB complex (*63*, *64*).

Transient and localized generation of $ONOO^-$ may also explain why the results presented here differ from those obtained in some but not all studies on the effects of reactive nitrogen species on NF-κB activity (*13*−*15*, *65*). High concentrations of $NO^\bullet$/$ONOO^-$ donors and/or prolonged exposure times inhibit NF-κB activity, e.g., 6−24 h (*15*). This contrasts with the transient generation of $ONOO^-$ achieved by a short IR exposure of cells or a single bolus addition of $ONOO^-$ (half-life of <1 s) to cell lysates. The transient nature of these treatments would be predictive of a higher degree of specificity in the nitration process. This is seen not only in terms of what tyrosines are nitrated but also in terms of whether other $ONOO^-$-induced oxidative events have occurred. Under the conditions used in these experiments, there is no evidence of nitration of either p65 or p50. There is also no evidence of the oxidation of either a cysteine or methionine. On the other hand, a single Y181F mutation was sufficient to block IR-stimulated NF-κB DNA binding activity and $ONOO^-$-induced dissociation of the NF-κB−IκBα complex. Combined with the effects of NOS inhibition and structural analysis, this is compelling evidence of a key role for Y181 nitration in IR stimulation of NF-κB activation.

An important characteristic of signal transduction pathways is their reversibility. The transient and relatively mild oxidative treatments used here may also have facilitated the apparent reversibility of the IR-stimulated IκBα tyrosine nitration. Although the mechanism of reversibility is not known, proteolytic degradation followed by resynthesis does not appear to be involved. This also is the case with the reversible nitration of mitochondrial proteins after hypoxia and reoxygenation (*62*). There are reports of denitrase activities in eukaryotic cells, but the underlying denitration mechanisms of eukaryotic cells remain undefined (*66*−*68*).

Because tyrosine nitration is not commonly studied in the context of signal transduction, it may be an undiscovered but important component for NF-κB activation by stimuli other than IR. A previous report that mitochondrion-generated superoxide anion and $ONOO^-$ are important for TNFα-stimulated NF-κB activation is interesting in this regard (*69*). Nitration and disruption of the interactions between Y181 of IκBα and p50 may be representative of a post-translational modification and structural motif critical for the stability of other protein complexes.

ACKNOWLEDGMENT

We thank Dr. Neal Scarsdale for the ^{13}C NMR studies.

SUPPORTING INFORMATION AVAILABLE

Highlighted region of the TOF mass spectrum of a tryptic digest of peroxynitrite-treated IκBα (Figure S1), MS/MS spectra for $[M + 3H]^{3+} = 814$ and $[M + 3H]^{3+} = 829$ (Figure S2), a gel showing NOS activity modulates NF-κB nuclear translocation (Figure S3), dipole moment vectors for tyrosine and nitrotyrosine (Figure S4), and mass spectroscopy results for IκBα protein (Table S1). This material is available free of charge via the Internet at http://pubs.acs.org.

REFERENCES

1. Ghosh, S., and Karin, M. (2002) Missing pieces in the NF-κB puzzle, *Cell 109* (Suppl.), S81−S96.
2. Beg, A. A., and Baldwin, A. S., Jr. (1993) The IκB proteins: Multifunctional regulators of Rel/NF-κB transcription factors, *Genes Dev. 7*, 2064−2070.
3. Criswell, T., Leskov, K., Miyamoto, S., Luo, G., and Boothman, D. A. (2003) Transcription factors activated in mammalian cells after clinically relevant doses of ionizing radiation, *Oncogene 22*, 5813−5827.
4. Pajonk, F., and McBride, W. H. (2001) The proteasome in cancer biology and treatment, *Radiat. Res. 156*, 447−459.
5. Raju, U., Gumin, G. J., Noel, F., and Tofilon, P. J. (1998) IκBα degradation is not a requirement for the X-ray-induced activation of nuclear factor κB in normal rat astrocytes and human brain tumour cells, *Int. J. Radiat. Biol. 74*, 617−624.
6. Liu, X., Huang, W., Li, C., Li, P., Yuan, J., Li, X., Qiu, X. B., Ma, Q., and Cao, C. (2006) Interaction between c-Abl and Arg tyrosine kinases and proteasome subunit PSMA7 regulates proteasome degradation, *Mol. Cell 22*, 317−327.
7. Hall, G., Singh, I. S., Hester, L., Hasday, J. D., and Rogers, T. B. (2005) Inhibitor-κB kinase-β regulates LPS-induced TNF-α production in cardiac myocytes through modulation of NF-κB p65 subunit phosphorylation, *Am. J. Physiol. 289*, H2103−H2111.
8. Sakurai, H., Chiba, H., Miyoshi, H., Sugita, T., and Toriumi, W. (1999) IκB kinases phosphorylate NF-κB p65 subunit on serine 536 in the transactivation domain, *J. Biol. Chem. 274*, 30353−30356.
9. Sasaki, C. Y., Barberi, T. J., Ghosh, P., and Longo, D. L. (2005) Phosphorylation of RelA/p65 on serine 536 defines an IκBα-independent NF-κB pathway, *J. Biol. Chem. 280*, 34538−34547.
10. Yang, F., Tang, E., Guan, K., and Wang, C. Y. (2003) IKKβ plays an essential role in the phosphorylation of RelA/p65 on serine 536 induced by lipopolysaccharide, *J. Immunol. 170*, 5630−5635.
11. Janssen-Heininger, Y. M., Macara, I., and Mossman, B. T. (1999) Cooperativity between oxidants and tumor necrosis factor in the activation of nuclear factor (NF)-κB: Requirement of Ras/mitogen-activated protein kinases in the activation of NF-κB by oxidants, *Am. J. Respir. Cell Mol. Biol. 20*, 942−952.

12. Levrand, S., Pesse, B., Feihl, F., Waeber, B., Pacher, P., Rolli, J., Schaller, M. D., and Liaudet, L. (2005) Peroxynitrite Is a Potent Inhibitor of NF-κB Activation Triggered by Inflammatory Stimuli in Cardiac and Endothelial Cell Lines, *J. Biol. Chem. 280*, 34878−34887.
13. Marshall, H. E., and Stamler, J. S. (2001) Inhibition of NF-κB by S-nitrosylation, *Biochemistry 40*, 1688−1693.
14. Matata, B. M., and Galinanes, M. (2002) Peroxynitrite is an essential component of cytokines production mechanism in human monocytes through modulation of nuclear factor-κB DNA binding activity, *J. Biol. Chem. 277*, 2330−2335.
15. Park, S. W., Huq, M. D., Hu, X., and Wei, L. N. (2005) Tyrosine nitration on p65: A novel mechanism to rapidly inactivate nuclear factor-κB, *Mol. Cell. Proteomics 4*, 300−309.
16. Kanai, A., Epperly, M., Pearce, L., Birder, L., Zeidel, M., Meyers, S., Greenberger, J., de Groat, W., Apodaca, G., and Peterson, J. (2004) Differing roles of mitochondrial nitric oxide synthase in cardiomyocytes and urothelial cells, *Am. J. Physiol. 286*, H13−H21.
17. Leach, J. K., Black, S. M., Schmidt-Ullrich, R. K., and Mikkelsen, R. B. (2002) Activation of constitutive nitric-oxide synthase activity is an early signaling event induced by ionizing radiation, *J. Biol. Chem. 277*, 15400−15406.
18. Leach, J. K., Van Tuyle, G., Lin, P. S., Schmidt-Ullrich, R., and Mikkelsen, R. B. (2001) Ionizing radiation-induced, mitochondria-dependent generation of reactive oxygen/nitrogen, *Cancer Res. 61*, 3894−3901.
19. Mikkelsen, R. B., and Wardman, P. (2003) Biological chemistry of reactive oxygen and nitrogen and radiation-induced signal transduction mechanisms, *Oncogene 22*, 5734−5754.
20. Barrett, D. M., Black, S. M., Todor, H., Schmidt-Ullrich, R. K., Dawson, K. S., and Mikkelsen, R. B. (2005) Inhibition of protein-tyrosine phosphatases by mild oxidative stresses is dependent on S-nitrosylation, *J. Biol. Chem. 280*, 14453−14461.
21. Phung, Y. T., and Black, S. M. (1999) Use of chimeric forms of neuronal nitric-oxide synthase as dominant negative mutants, *IUBMB Life 48*, 333−338.
22. Amorino, G. P., Hamilton, V. M., Valerie, K., Dent, P., Lammering, G., and Schmidt-Ullrich, R. K. (2002) Epidermal growth factor receptor dependence of radiation-induced transcription factor activation in human breast carcinoma cells, *Mol. Biol. Cell 13*, 2233−2244.
23. Shevchenko, A., Wilm, M., Vorm, O., and Mann, M. (1996) Mass spectrometric sequencing of proteins silver-stained polyacrylamide gels, *Anal. Chem. 68*, 850−858.
24. Schmidt, M. W., Baldridge, K. K., Boatz, J. A., Elbert, S. T., Gordon, M. S., Jensen, J. H., Koseki, S., Matsunaga, N., Nguyen, K. A., Su, S. J., Windus, T. L., Dupuis, M., and Montgomery, J. A. (1993) General atomic and molecular electronic structure system, *J. Comput. Chem. 14*, 1347−1363.
25. MacKerell, A. D., Bashford, D., Bellott, M., Dunbrack, R. L., Evanseck, J. D., Field, M. J., Fischer, S., Gao, J., Guo, H., Ha, S., Joseph-McCarthy, D., Kuchnir, L., Kuczera, K., Lau, F. T. K., Mattos, C., Michnick, S., Ngo, T., Nguyen, D. T., Prodhom, B., Reiher, W. E., Roux, B., Schlenkrich, M., Smith, J. C., Stote, R., Straub, J., Watanabe, M., Wiorkiewicz-Kuczera, J., Yin, D., and Karplus, M. (1998) All-Atom Empirical Potential for Molecular Modeling and Dynamics Studies of Proteins, *J. Phys. Chem. B 102*, 3586−3616.
26. Humphrey, W., Dalke, A., and Schulten, K. (1996) VMD: Visual molecular dynamics, *J. Mol. Graphics 14*, 27−38.
27. Kale, L., Skeel, R., Bhandarkar, M., Brunner, R., Gursoy, A., Krawetz, N., Phillips, J., Shinozaki, A., Varadarajan, K., and Schulten, K. (1999) NAMD2: Greater Scalability for Parallel Molecular Dynamics, *J. Comput. Phys. 151*, 283−312.
28. Jacobs, M. D., and Harrison, S. C. (1998) Structure of an IκBα/NF-κB complex, *Cell 95*, 749−758.
29. Huxford, T., Huang, D. B., Malek, S., and Ghosh, G. (1998) The crystal structure of the IκBα/NF-κB complex reveals mechanisms of NF-κB inactivation, *Cell 95*, 759−770.
30. Amadasi, A., Spyrakis, F., Cozzini, P., Abraham, D. J., Kellogg, G. E., and Mozzarelli, A. (2006) Mapping the energetics of water-protein and water-ligand interactions with the "natural" HINT forcefield: Predictive tools for characterizing the roles of water in biomolecules, *J. Mol. Biol. 358*, 289−309.
31. Kellogg, G. E., Fornabaio, M., Chen, D. L., Abraham, D. J., Spyrakis, F., Cozzini, P., and Mozzarelli, A. (2006) Tools for building a comprehensive modeling system for virtual screening under real biological conditions: The Computational Titration algorithm, *J. Mol. Graphics Modell. 24*, 434−439.
32. Cozzini, P., Fornabaio, M., Marabotti, A., Abraham, D. J., Kellogg, G. E., and Mozzarelli, A. (2004) Free energy of ligand binding to protein: Evaluation of the contribution of water molecules by computational methods, *Curr. Med. Chem. 11*, 3093−3118.
33. Cozzini, P., Fornabaio, M., Marabotti, A., Abraham, D. J., Kellogg, G. E., and Mozzarelli, A. (2002) Simple, intuitive calculations of free energy of binding for protein-ligand complexes. 1. Models without explicit constrained water, *J. Med. Chem. 45*, 2469−2483.
34. Kellogg, G. E., Burnett, J. C., and Abraham, D. J. (2001) Very empirical treatment of solvation and entropy: A force field derived from log Po/w, *J. Comput.-Aided Mol. Des. 15*, 381−393.
35. Marabotti, A., Balestreri, L., Cozzini, P., Mozzarelli, A., Kellogg, G. E., and Abraham, D. J. (2000) HINT predictive analysis of binding between retinol binding protein and hydrophobic ligands, *Bioorg. Med. Chem. Lett. 10*, 2129−2132.
36. Rodel, F., Hantschel, M., Hildebrandt, G., Schultze-Mosgau, S., Rodel, C., Herrmann, M., Sauer, R., and Voll, R. E. (2004) Dose-dependent biphasic induction and transcriptional activity of nuclear factor κB (NF-κB) in EA.hy.926 endothelial cells after low-dose X-irradiation, *Int. J. Radiat. Biol. 80*, 115−123.
37. Ueda, T., Akiyama, N., Sai, H., Oya, N., Noda, M., Hiraoka, M., and Kizaka-Kondoh, S. (2001) c-IAP2 is induced by ionizing radiation through NF-κB binding sites, *FEBS Lett. 491*, 40−44.
38. Wang, T., Hu, Y. C., Dong, S., Fan, M., Tamae, D., Ozeki, M., Gao, Q., Gius, D., and Li, J. J. (2005) Co-activation of ERK, NF-κB, and GADD45β in response to ionizing radiation, *J. Biol. Chem. 280*, 12593−12601.
39. Hoffmann, A., Levchenko, A., Scott, M. L., and Baltimore, D. (2002) The IκB-NF-κB signaling module: Temporal control and selective gene activation, *Science 298*, 1241−1245.
40. Nelson, D. E., Ihekwaba, A. E., Elliott, M., Johnson, J. R., Gibney, C. A., Foreman, B. E., Nelson, G., See, V., Horton, C. A., Spiller, D. G., Edwards, S. W., McDowell, H. P., Unitt, J. F., Sullivan, E., Grimley, R., Benson, N., Broomhead, D., Kell, D. B., and White, M. R. (2004) Oscillations in NF-κB signaling control the dynamics of gene expression, *Science 306*, 704−708.
41. Imbert, V., Rupec, R. A., Livolsi, A., Pahl, H. L., Traenckner, E. B., Mueller-Dieckmann, C., Farahifar, D., Rossi, B., Auberger, P., Baeuerle, P. A., and Peyron, J. F. (1996) Tyrosine phosphorylation of IκB-α activates NF-κB without proteolytic degradation of IκB-α, *Cell 86*, 787−798.
42. Bagnasco, P., MacMillan-Crow, L. A., Greendorfer, J. S., Young, C. J., Andrews, L., and Thompson, J. A. (2003) Peroxynitrite modulates acidic fibroblast growth factor (FGF-1) activity, *Arch. Biochem. Biophys. 419*, 178−189.
43. Batthyany, C., Souza, J. M., Duran, R., Cassina, A., Cervenansky, C., and Radi, R. (2005) Time course and site(s) of cytochrome c tyrosine nitration by peroxynitrite, *Biochemistry 44*, 8038−8046.
44. Huxford, T., Mishler, D., Phelps, C. B., Huang, D. B., Sengchanthalangsy, L. L., Reeves, R., Hughes, C. A., Komives, E. A., and Ghosh, G. (2002) Solvent exposed non-contacting amino acids play a critical role in NF-κB/IκBα complex formation, *J. Mol. Biol. 324*, 587−597.
45. Takada, Y., Mukhopadhyay, A., Kundu, G. C., Mahabeleshwar, G. H., Singh, S., and Aggarwal, B. B. (2003) Hydrogen peroxide activates NF-κB through tyrosine phosphorylation of IκBα and serine phosphorylation of p65: Evidence for the involvement of IκBα kinase and Syk protein-tyrosine kinase, *J. Biol. Chem. 278*, 24233−24241.
46. Burow, M. E., Weldon, C. B., Tang, Y., Navar, G. L., Krajewski, S., Reed, J. C., Hammond, T. G., Clejan, S., and Beckman, B. S. (1998) Differences in susceptibility to tumor necrosis factor α-induced apoptosis among MCF-7 breast cancer cell variants, *Cancer Res. 58*, 4940−4946.
47. Abraham, D. J., Kellogg, G. E., Holt, J. M., and Ackers, G. K. (1997) Hydropathic analysis of the non-covalent interactions between molecular subunits of structurally characterized hemoglobins, *J. Mol. Biol. 272*, 613−632.
48. Burnett, J. C., Kellogg, G. E., and Abraham, D. J. (2000) Computational methodology for estimating changes in free energies of biomolecular association upon mutation. The importance of bound water in dimer-tetramer assembly for β37 mutant hemoglobins, *Biochemistry 39*, 1622−1633.
49. Burnett, J. C., Botti, P., Abraham, D. J., and Kellogg, G. E. (2001) Computationally accessible method for estimating free energy changes resulting from site-specific mutations of biomolecules:

Systematic model building and structural/hydropathic analysis of deoxy and oxy hemoglobins, *Proteins 42*, 355−377.
50. Tawfik, D. S., Chap, R., Eshhar, Z., and Green, B. S. (1994) pH on-off switching of antibody-hapten binding by site-specific chemical modification of tyrosine, *Protein Eng. 7*, 431−434.
51. Oneda, H., and Inouye, K. (2003) Effect of nitration on the activity of bovine erythrocyte Cu,Zn-superoxide dismutase (BESOD) and a kinetic analysis of its dimerization-dissociation reaction as examined by subunit exchange between the native and nitrated BESODs, *J. Biochem. 134*, 683−690.
52. Li, N., and Karin, M. (1998) Ionizing radiation and short wavelength UV activate NF-κB through two distinct mechanisms, *Proc. Natl. Acad. Sci. U.S.A. 95*, 13012−13017.
53. Hodara, R., Norris, E. H., Giasson, B. I., Mishizen-Eberz, A. J., Lynch, D. R., Lee, V. M., and Ischiropoulos, H. (2004) Functional consequences of α-synuclein tyrosine nitration: Diminished binding to lipid vesicles and increased fibril formation, *J. Biol. Chem. 279*, 47746−47753.
54. Ischiropoulos, H., and Gow, A. (2005) Pathophysiological functions of nitric oxide-mediated protein modifications, *Toxicology 208*, 299−303.
55. Ji, Y., Neverova, I., Van Eyk, J. E., and Bennett, B. M. (2006) Nitration of tyrosine 92 mediates the activation of rat microsomal glutathione S-transferase by peroxynitrite, *J. Biol. Chem. 281*, 1986−1991.
56. Knyushko, T. V., Sharov, V. S., Williams, T. D., Schoneich, C., and Bigelow, D. J. (2005) 3-Nitrotyrosine modification of SERCA2a in the aging heart: A distinct signature of the cellular redox environment, *Biochemistry 44*, 13071−13081.
57. Radi, R. (2004) Nitric oxide, oxidants, and protein tyrosine nitration, *Proc. Natl. Acad. Sci. U.S.A. 101*, 4003−4008.
58. Kawai, H., Nie, L., and Yuan, Z. M. (2002) Inactivation of NF-κB-dependent cell survival, a novel mechanism for the proapoptotic function of c-Abl, *Mol. Cell. Biol. 22*, 6079−6088.
59. Mallozzi, C., Di Stasi, A. M., and Minetti, M. (2001) Nitrotyrosine mimics phosphotyrosine binding to the SH2 domain of the src family tyrosine kinase lyn, *FEBS Lett. 503*, 189−195.
60. Ischiropoulos, H. (2003) Biological selectivity and functional aspects of protein tyrosine nitration, *Biochem. Biophys. Res. Commun. 305*, 776−783.
61. Sacksteder, C. A., Qian, W. J., Knyushko, T. V., Wang, H., Chin, M. H., Lacan, G., Melega, W. P., Camp, D. G., II, Smith, R. D., Smith, D. J., Squier, T. C., and Bigelow, D. J. (2006) Endogenously Nitrated Proteins in Mouse Brain: Links to Neurodegenerative Disease, *Biochemistry 45*, 8009−8022.
62. Aulak, K. S., Koeck, T., Crabb, J. W., and Stuehr, D. J. (2004) Dynamics of protein nitration in cells and mitochondria, *Am. J. Physiol. 286*, H30−H38.
63. Bottero, V., Rossi, F., Samson, M., Mari, M., Hofman, P., and Peyron, J. F. (2001) Iκb-α, the NF-κB inhibitory subunit, interacts with ANT, the mitochondrial ATP/ADP translocator, *J. Biol. Chem. 276*, 21317−21324.
64. Cogswell, P. C., Kashatus, D. F., Keifer, J. A., Guttridge, D. C., Reuther, J. Y., Bristow, C., Roy, S., Nicholson, D. W., and Baldwin, A. S., Jr. (2003) NF-κB and IκBα are found in the mitochondria. Evidence for regulation of mitochondrial gene expression by NF-κB, *J. Biol. Chem. 278*, 2963−2968.
65. Reynaert, N. L., Ckless, K., Korn, S. H., Vos, N., Guala, A. S., Wouters, E. F., van der Vliet, A., and Janssen-Heininger, Y. M. (2004) Nitric oxide represses inhibitory κB kinase through S-nitrosylation, *Proc. Natl. Acad. Sci. U.S.A. 101*, 8945−8950.
66. Gorg, B., Qvartskhava, N., Voss, P., Grune, T., Haussinger, D., and Schliess, F. (2007) Reversible inhibition of mammalian glutamine synthetase by tyrosine nitration, *FEBS Lett. 581*, 84−90.
67. Irie, Y., Saeki, M., Kamisaki, Y., Martin, E., and Murad, F. (2003) Histone H1.2 is a substrate for denitrase, an activity that reduces nitrotyrosine immunoreactivity in proteins, *Proc. Natl. Acad. Sci. U.S.A. 100*, 5634−5639.
68. Kuo, W. N., Kanadia, R. N., Shanbhag, V. P., and Toro, R. (1999) Denitration of peroxynitrite-treated proteins by 'protein nitratases' from rat brain and heart, *Mol. Cell. Biochem. 201*, 11−16.
69. Higuchi, M., Manna, S. K., Sasaki, R., and Aggarwal, B. B. (2002) Regulation of the activation of nuclear factor κB by mitochondrial respiratory function: Evidence for the reactive oxygen species-dependent and -independent pathways, *Antioxid. Redox Signaling 4*, 945−955.

BI701107Z